

Efficient eNB Deployment Strategy for Heterogeneous Cells in 4G LTE Systems

You-Chiun Wang and Chien-An Chuang

Abstract—Base station deployment is an important issue in cellular communication systems because it determines the cost to construct and maintain a system and also the service quality to users. Conventional 2G and 3G systems assume that base stations are identical in the sense that they have the similar coverage range. For 4G systems, LTE introduces the concept of heterogeneous base stations (also called *eNBs*), which supports different sizes of coverage range. Given the user distribution and demands in a service area, the problem of deploying heterogeneous *eNBs* is NP-hard. Therefore, we propose a four-stage *eNB* deployment strategy to efficiently solve the problem. Our strategy first employs a geometric approach to provide the basic coverage to the service area. Then, it adaptively adjusts the cell range to satisfy the user demands under the power and bandwidth constraints on each *eNB*. Simulation results verify that the proposed strategy not only significantly saves the system cost, but also reduces the power consumption while balances the traffic loads of *eNBs*.

Index Terms—base station deployment, cell planning, heterogeneous network (HetNet), long term evolution (LTE), network management.

1 INTRODUCTION

THE market of intelligent, hand-held communication devices such as mobile phones and tablet computers keeps growing year by year. Except for the basic voice communication, various wireless multimedia services with large bandwidth demand such as video streaming and teleconference services should be also supported by network operators. To follow this trend, ITU (International Telecommunication Union) defines IMT-A (International Mobile Telecommunications-Advanced) requirements for the current 4G communication systems [1]. Specifically, the target peak data rate (for total users) is 1 Gbps in the downlink and 500 Mbps in the uplink. Therefore, 3GPP (the third Generation Partnership Project) specifies *long term evolution (LTE)* and its advanced version, *LTE-A*, in order to meet the above IMT-A requirements [2].

For a cellular communication system, one critical issue is to determine the locations of base stations (BSs), also known as *BS deployment*, so as to provide the maximum service coverage with the minimum system cost. Existing 2G and 3G systems usually consider BSs with similar hardware characteristics such as antennas and power levels. A network operator may first predict where BSs should be located in theory or by simulations so that not only the service coverage is increased but also the interference between adjacent cells is reduced. Thus, BSs are often planned to be deployed in a regular fashion [3]. Then, BSs are practically deployed wherever the operator can acquire rights to purchase and install sites. However, because all cells have the similar coverage range, the above deployment may not work well when users request large traffic demands or some of them congregate in certain small regions (called *hotspots*, such as coffee shops or airports) [4].

In LTE, a BS is also called an *E-UTRAN NodeB* (or *eNB* shortly). Depending on their coverage range, LTE defines four types of *eNBs* (from large range to small range): *macro-cell*, *micro-cell*, *pico-cell*, and *femto-cell eNBs*. Only femto-cell *eNBs* can be user-installed, whereas other *eNBs* are operator-

TABLE 1: Comparison on LTE *eNBs*.

eNB	transmission power	cell size	users supported
macro-cell	20 W – 160 W	> 1 km	> micro-cell
micro-cell	2 W – 20 W	250 m – 1 km	> pico-cell
pico-cell	250 mW – 2 W	100 m – 300 m	32
femto-cell	10 mW – 200 mW	10 m – 50 m	8

[Unit] m: meter, km: kilometer, W: watt, mW: milliwatt

[Notice] The typical transmission power of a macro-cell *eNB* is 40 W.

installed. Table 1 compares these four types of *eNBs* [5], [6]. By allowing different types of *eNBs* to coexist in the same service area, LTE introduces the concept of *heterogeneous network (HetNet)* to address the above large user-demand and hotspot issues. In particular, macro-cell *eNBs* serve as the backbone to provide signal coverage in large geographic regions. Then, micro-cell and pico-cell *eNBs* can provide service to hotspots or fill those ‘uncovered holes’ left by macro-cells. Finally, users can install their own femto-cell *eNBs* to improve the signal quality.

The *eNB* deployment issue in LTE HetNets is also addressed in the literature, but most of relevant research discusses only the combination of large macro-cell and small femto-cell (or pico-cell) *eNBs*. This motivates us to study the *eNB deployment with the minimum cost (EDMC) problem*, where three types of operator-installed *eNBs* are considered (that is, macro-cell, micro-cell, and pico-cell *eNBs*). Given the distribution of *LTE user equipments (UEs)* and their traffic demands, the EDMC problem asks how to deploy different *eNBs* to meet the demands of all *UEs* such that the total system cost is minimized. The problem is NP-hard, so we develop an efficient four-stage strategy. Our idea is to first use large cells to provide basic coverage to every *UE*. Then, for each cell, our strategy checks whether the *eNB* has sufficient power and bandwidth resource to support all *UEs* in the cell. If not, the cell range is shrunk accordingly. Finally, small cells are added to strengthen the network deployment.

The contributions of this paper are threefold. First, the proposed EDMC problem considers all types of operator-installed *eNBs*, whereas many research efforts disregard micro-cell *eNBs*. Our EDMC solution thus helps support more flex-

ible network deployment. In addition, we consider path loss, shadowing, multipath fading, and environmental noise, which can model LTE communication channels more realistically. Second, we develop an efficient eNB deployment strategy by considering not only the positions of UEs but also the power and bandwidth constraints on each eNB to meet UEs' traffic demands. Furthermore, several research issues of our strategy such as the fluctuations in UE density, impact of uplink transmission, and cell interference are also discussed in the paper. Third, we design four different scenarios of UE distributions in the simulations to evaluate the performance of our eNB deployment strategy. Experimental results demonstrate that our strategy can significantly save the overall system cost, reduce the power consumption of macro-cell eNBs, and deal out the load of each macro-cell eNB to its nearby small-cell eNBs.

The rest of this paper is organized as follows. The next section discusses the related work. Section 3 first addresses the eNB parameters and the fading and noise models used to describe an LTE communication channel. Then, the section formally defines the EDMC problem. Section 4 presents our eNB deployment strategy to the EDMC problem and Section 5 investigates some research issues in the proposed strategy. Experimental results are shown in Section 6. Finally, we give the conclusion and future work in Section 7.

2 RELATED WORK

BS deployment has been widely discussed in 2G and 3G communication systems. For 2G systems, many research efforts [7]–[10] consider two-phase BS deployment. In phase 1, they select a set of candidate locations to place macro-cell BSs in order to meet the given capacity demand such that the system cost can be reduced. Then, phase 2 aims at allocating frequency channels to BSs such that the interference between two adjacent cells can be eliminated while user QoS (quality of service) can be satisfied. On the other hand, 3G systems do not require the above phase 2 since all BSs share the same frequency spectrum. Therefore, 3G BS deployment [11]–[14] focuses on selecting the locations of BSs and adjusting their transmission power, with the consideration of cell interference. However, these studies only consider identical macro-cell BSs and thus their results may not be directly applied to wireless HetNets. Ting et al. [15] propose a multi-objective variable-length genetic algorithm to address BS deployment in a wireless HetNet containing both WiMAX and WiFi BSs, where the goal is to maximize the network coverage while minimizing the system cost. However, only two types of BSs are considered and the BS planning model aims at the map instead of the user distribution. The work of [16] proposes a *budgeted cell planning problem* for cellular networks with small cells, and its objective is to maximize the number of traffic demand nodes whose required rates are fully satisfied under the budget constraint. The problem is proven to be NP-hard and an approximation algorithm which yields an $(e - 1)/2e$ fraction of the optimum is developed. Obviously, [16] has different objective with our work.

Several research efforts also investigate the LTE eNB deployment issue. By measuring the commercial GSM (Global System for Mobile Communications) live traffic to capture the spatial distribution of UEs, [17] can assess LTE downlink inter-cell interference and thus determine where to deploy macro-cell eNBs. However, it does not consider LTE HetNets. Both

[18] and [19] discuss how to efficiently add femto-cell eNBs in existing LTE macro-cells in order to improve the service coverage and network capacity. As mentioned earlier, femto-cell eNB are usually user-installed for private usage. Some studies consider LTE HetNets with the coexistence of macro-cells and pico-cells. Specifically, the work of [20] determines the location, transmission power, and antenna tilt of each pico-cell eNB with the help of *CRE (cell range expansion)* and *TDM-ICIC (time domain multiplexing inter-cell interference coordination)* techniques, which can balance macro-cell eNBs' loads and mitigate their interference, respectively. Barbera et al. [3] evaluate the effect of different pico-cell eNB deployment and user mobility patterns on UE handover between LTE cells. Given the deployment of macro-cell and pico-cell eNBs, [21] seeks to 'switch off' some macro-cell eNBs to save the overall energy. In this case, the nearby pico-cell eNBs will be responsible for serving UEs so that there is no loss of network capacity. Apparently, these studies have different objectives with our EDMC problem. Zhao et al. [22], [23] consider the minimum-cost cell planning problem in an LTE HetNet, which asks how to select a subset of candidate eNB sites (including macro-cell and pico-cell eNBs) in order to minimize the overall deployment cost and satisfy the rate requirements of all UEs. The problem is NP-hard and they thus develop an $O(\log R)$ -approximation solution, where R is the maximum achievable capacity of eNBs. Since the EDMC problem considers not only macro-cells and pico-cells but also micro-cells, it is more difficult than the above problem. Thus, the EDMC problem is NP-hard and we will propose an efficient eNB deployment strategy based on the distribution of UEs and their traffic demands.

3 SYSTEM MODEL

In this section, we first present the parameters of eNBs used in our deployment strategy. Then, we define the fading effect and noise to model an LTE communication channel and finally formulate the EDMC problem.

3.1 eNB Parameters

We aim at the deployment of operator-installed eNBs in the service area. Let P_{macro} , P_{micro} , and P_{pico} be the typical transmission power of a macro-cell, micro-cell, and pico-cell eNB, respectively. According to the transmission power, we can estimate the communication range of a macro-cell, micro-cell, and pico-cell eNB (respectively denoted by R_{macro} , R_{micro} and R_{pico}). Apparently, higher transmission power implies larger communication range (and thus a larger cell size). From Table 1, we can obtain that $P_{macro} \geq P_{micro} \geq P_{pico}$ and therefore $R_{macro} \geq R_{micro} \geq R_{pico}$.

Although the communication range is tightly coupled with the transmission power, we still separately define these two parameters due to two reasons. First, both transmission power and communication range are two fundamental eNB characteristics, where some eNB manufacturers also indicate these two parameters in their products [6], [24]. (Table 1 also lists the common transmission power and communication range of different LTE eNBs.) Second, separately defining transmission power and communication range can help facilitate the deployment process. In particular, we can easily 'filter' out those UEs outside a cell by using the communication range. Then, each eNB can examine only the UEs inside its cell and

determine whether it has sufficient power to serve these UEs. In this way, the eNB does not need to examine every UE in the service area.

On the other hand, let us denote by B_{macro}^{DL} , B_{micro}^{DL} , and B_{pico}^{DL} the total downlink bandwidth supported by a macro-cell, micro-cell, and pico-cell eNB, respectively. These bandwidth parameters depend on the *component carriers* possessed by an eNB. The LTE standard allows a component carrier to have the bandwidth of 1.4 MHz, 3 MHz, 5 MHz, 10 MHz, 15 MHz, and 20 MHz. Based on the operating frequency band of an eNB¹, we can obtain its component carriers and thus estimate the corresponding bandwidth. In addition, we define the cost to install and maintain a macro-cell, micro-cell, and pico-cell eNB by the notations C_{macro} , C_{micro} , and C_{pico} , respectively. According to [25], it is common that $C_{macro} > C_{micro} > C_{pico}$.

3.2 Fading and Noise Models

Generally speaking, a transmission signal will be affected by three major types of fading: *path loss*, *slow fading* (also called *shadowing fading*), and *fast fading* (also called *multipath fading*). These fading effects are important to model a wireless channel. Specifically, path loss is the power attenuation of a signal in the propagation environment when it travels from the transmitter to the receiver. According to the LTE standard (Release 9) [26], we employ the *log-distance model* to estimate path loss. In particular, the path-loss effect of a macro-cell is calculated by

$$PL_{macro} = 128.1 + 37.6 \log_{10}(r), \quad (1)$$

where r is the distance between a UE and the eNB (in kilometers). For both micro-cells and pico-cells, the path-loss effect is measured by

$$PL_{small} = 140.7 + 36.7 \log_{10}(r). \quad (2)$$

On the other hand, slow fading is the obstruction encountered by a signal when some objects (such as buildings or trees) block its transmission path. It will result in random variation in the signal's amplitude and thus cannot be simply modeled by path loss. Therefore, we adopt the popular *log-normal shadowing model* [27] to estimate slow fading. Specifically, let us denote by \mathcal{S} the random variable of the ratio of the power transmitted to the power received in decibel (dB) scale, where the received signal power is attenuated by slow fading. Then, the probability distribution of \mathcal{S} can be expressed by

$$p(\mathcal{S}) = \frac{1}{\sqrt{2\pi}\sigma} \exp\left(-\frac{(\mathcal{S} - \mu)^2}{2\sigma^2}\right), \quad (3)$$

where μ and σ are the mean and standard deviation of \mathcal{S} in dB, respectively. The LTE standard suggests setting $\mu = 0$ dB (that is, zero mean), and $\sigma = 10$ dB and 6 dB for a macro-cell and micro-cell/pico-cell eNB, respectively.

Fast fading is caused by the reception of a signal at the receiver from more than one path. *Jakes fading model* [28] and its variations are widely used to evaluate such an effect. They consider a moving UE that receives k rays with equal signal strength. Each ray i arrives at an angle of $\alpha_i = 2\pi i/k$ and encounters a Doppler shift of $\omega_i = \omega_{\max} \cos(\alpha_i)$, where $\omega_{\max} = 2\pi f v/c$ is the maximum Doppler shift which will be

1. ITU totally defines 44 frequency bands for LTE operation. Each network operator has to apply for some of them (usually two to three bands) before operating. Therefore, which bands are operated by an eNB is actually known in advance.

encountered at receiver speed of v , carrier frequency f , and speed of light c . Then, the signal waveform received by the UE can be expressed by a function of time t :

$$g(t) = \Upsilon \left(\frac{1}{\sqrt{2}} (\cos(\alpha) + j \sin(\alpha)) \cdot \cos(\omega_{\max} t + \theta_0) + \sum_{i=1}^N (\cos(\beta_i) + j \sin(\beta_i)) \cdot \cos(\omega_i t + \theta_i) \right), \quad (4)$$

where Υ is a normalization constant and $N = (k/2 - 1)/2$. In Eq. (4), the variables j , α , β_i , and θ_i are the model parameters.

Except for the fading effects, the thermal noise in the environment will also affect the transmission signal. To simulate such noise, we employ the *additive white Gaussian noise (AWGN)* model [29] as suggested by the LTE standard, where the power spectral density of AWGN is set to -174 dBm/Hz (decibel-milliwatt per hertz).

3.3 The EDMC Problem

Let \hat{E} be the set of all possible sites on which the network operator acquires rights to deploy eNBs in the service area. The EDMC problem seeks to select a subset of \hat{E} to deploy eNBs with the minimum cost so as to satisfy the traffic demands of a set of UEs \hat{U} , where the total amount of power and bandwidth of each eNB allocated to its UEs cannot exceed the given thresholds (defined in Section 3.1). Specifically, let e_i denote the selection variable of an eNB _{i} , where

$$e_i = \begin{cases} 1 & \text{eNB}_i \text{ is selected for deployment,} \\ 0 & \text{otherwise,} \end{cases} \quad \forall i \in \hat{E}.$$

Then, the EDMC problem can be formulated as follows:

$$\min_{e_i, p_{i,j}, b_{i,j}} \sum_{i \in \hat{E}} e_i C_i, \quad C_i \in \{C_{macro}, C_{micro}, C_{pico}\} \quad (5)$$

$$\text{such that } \sum_{u_j \in \hat{U}} b_{i,j}^{DL} \leq e_i B_i^{DL},$$

$$\forall i \in \hat{E}, B_i^{DL} \in \{B_{macro}^{DL}, B_{micro}^{DL}, B_{pico}^{DL}\} \quad (6)$$

$$\sum_{u_j \in \hat{U}} p_{i,j} \leq e_i P_i,$$

$$\forall i \in \hat{E}, P_i \in \{P_{macro}, P_{micro}, P_{pico}\} \quad (7)$$

$$\sum_{i \in \hat{E}} r_{i,j}^{DL} \geq r_j^{DL}, \quad \forall u_j \in \hat{U}, \quad (8)$$

$$b_{i,j}^{DL} \geq 0, p_{i,j} \geq 0, \quad \forall i \in \hat{E}, u_j \in \hat{U}, \quad (9)$$

under the channel constraints defined in Section 3.2, where C_i , B_i^{DL} , and P_i are respectively the cost, downlink bandwidth, and transmission power of eNB _{i} (depending on its type); $p_{i,j}$, $b_{i,j}^{DL}$, $r_{i,j}^{DL}$ are respectively the downlink power, bandwidth, and data rate that eNB _{i} allocates to a UE u_j ; r_j^{DL} is the expected downlink traffic demand of u_j . Here, Eq. (5) is the objective function, which wants to minimize the overall system cost. Eqs. (6) and 7 respectively indicate that the total bandwidth and power of eNB _{i} allocated to all UEs in its cell cannot exceed the thresholds B_i^{DL} and P_i . Eq. (8) means that the deployment of eNBs should satisfy the expected downlink traffic demand of each UE. Eq. (9) shows that the allocation of power and bandwidth for UEs is non-negative.

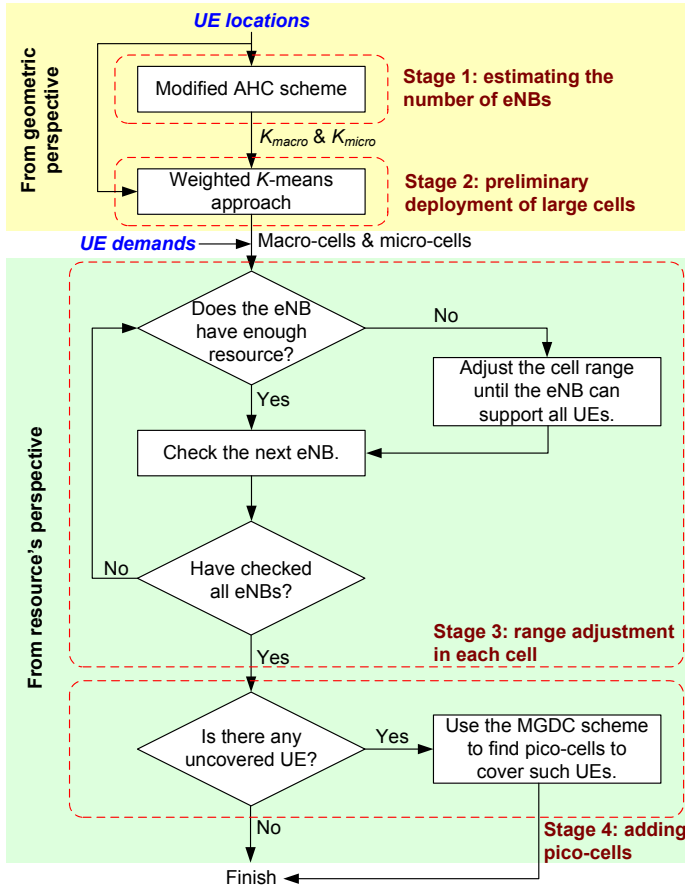


Fig. 1: The flow diagram of our proposed eNB deployment strategy.

4 THE PROPOSED ENB DEPLOYMENT STRATEGY

Given the locations and traffic demands of UEs, Fig. 1 presents the flow diagram of our eNB deployment strategy. It consists of four major stages:

- **[Stage 1] Estimating the number of eNBs:** By taking the locations of UEs as the input, this stage will calculate how many macro-cells and micro-cells (respectively denoted by K_{macro} and K_{micro}) are necessary to provide the basic coverage to the service area. To do so, we develop a ‘modified’ *agglomerative hierarchical clustering (AHC)* scheme to compute both K_{macro} and K_{micro} .
- **[Stage 2] Preliminary deployment of large cells:** Given both K_{macro} and K_{micro} values from stage 1 and the locations of UEs, this stage then gives ‘preliminary’ deployment of macro-cells and micro-cells to cover all UEs in the service area. This is achieved by a novel *weighted K-means approach*.
- **[Stage 3] Range adjustment in each cell:** The previous stage does not guarantee to meet the traffic demands of UEs. Therefore, we check whether each eNB has sufficient resource (that is, power and bandwidth) to support all of its UEs. If not, we gradually ‘shrink’ the cell range by removing outer UEs, until the eNB can satisfy the traffic demands of residual UEs.
- **[Stage 4] Adding pico-cells:** If the above stage lets some UEs become *uncovered*, we then add pico-cells in the service area to cover them. Since all UEs are

eventually covered by the deployed eNBs, our strategy thus finishes.

Next, we present the detailed design of each stage and then discuss the rationale of our eNB deployment strategy.

4.1 Stage 1: Estimating the Number of eNBs

According to Fig. 1, this stage takes the locations of UEs as the input to calculate the number of macro-cells and micro-cells used to cover all UEs in the service area. This is based on the two parameters R_{macro} and R_{micro} , which can be respectively derived from P_{macro} and P_{micro} . To do so, we modify the AHC scheme [30] to ‘recursively’ groups UEs into clusters by the following steps:

- 1) Each UE $u_i \in \hat{U}$ is initially treated as a single cluster c_i .
- 2) Then, we combine two clusters c_i and c_j such that they have the minimum *inter-cluster distance* $d(c_i, c_j)$, which is defined by the shortest distance between two UEs $u_a \in c_i$ and $u_b \in c_j$.
- 3) We repeat step 2 until all UEs are grouped into one single cluster.

Fig. 2 (a) and (b) together present an example, where each UE u_i is treated as a cluster c_i in the beginning, $i = 1..6$. Since both $d(c_2, c_3)$ and $d(c_4, c_5)$ have the minimum value, two clusters $c_7 = \{c_2, c_3\}$ and $c_8 = \{c_4, c_5\}$ are found. Then, c_6 is combined with c_8 (due to the smallest inter-cluster distance) and thus a new cluster c_9 is generated. Following the similar manner, both clusters c_{10} and c_{11} are calculated. From Fig. 2(b), it can be observed that the clustering result will form a binary tree, where each cluster (except for the leaf clusters) must have two child clusters.

Then, according to the above clustering result, we can calculate how many macro-cells and micro-cells are required to cover all UEs in a *top-down* manner. In particular, we initially set both K_{macro} and K_{micro} to zero and start from the root cluster. For each cluster being checked, say, c_i , we conduct the following operations:

- If a micro-cell is enough to cover all UEs in c_i , we then add K_{micro} by one. Specifically, let $D(c_i)$ denote the *diameter* of c_i , which is calculated by the Euclidean distance between the two farthest UEs in c_i . When $D(c_i) \leq R_{micro}$, then one micro-cell is able to cover all UEs in c_i .
- When the above operation fails, we then check if a macro-cell is enough to cover all UEs in c_i . In particular, if $D(c_i) \leq R_{macro}$, all UEs in c_i can be covered by one macro-cell and thus we increase K_{macro} by one.
- Otherwise, we do the checks for c_i ’s two child clusters.

We use Fig. 2 (b) and (c) to illustrate the above checks. In the beginning, we check the root cluster c_{11} . Because no single macro-cell can cover all UEs in c_{11} , we should check its child clusters c_1 and c_{10} . For c_1 , we can use just one micro-cell to cover it (because there is only one UE u_1 in c_1). On the other hand, we cannot use one macro-cell to cover all UEs in cluster c_{10} , so we go through the tree and check the two child clusters c_7 and c_9 . In this case, both c_7 and c_9 can be individually covered by one macro-cell. Therefore, we can estimate that $K_{macro} = 2$ and $K_{micro} = 1$ in this example.

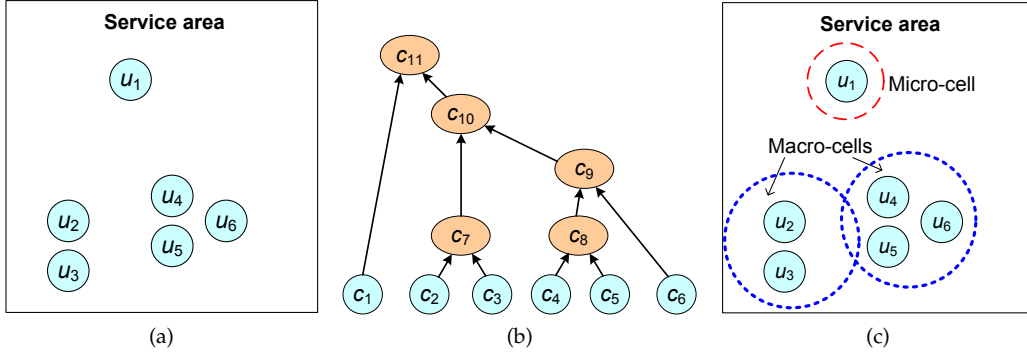


Fig. 2: The modified AHC scheme: (a) the distribution of UEs in the service area, (b) the clustering result (in a binary tree), and (c) calculating the number of macro-cells and micro-cells used to cover all UEs.

4.2 Stage 2: Preliminary Deployment of Large Cells

Given the result from stage 1, we then deploy K_{macro} macro-cells and K_{micro} micro-cells in the service area, as presented in Fig. 1. The idea is to divide UEs according to their geographic relationships so that each group of UEs can be covered by either one macro-cell or micro-cell. K -means [31] is a popular approach to achieve such a mission, but the traditional K -means approach does not take heterogeneous cells into account. Therefore, we develop a *weighted K-means approach* to provide preliminary deployment of macro-cells and micro-cells:

- 1) Initially, we partition all UEs in \hat{U} into $(K_{macro} + K_{micro})$ groups. For each group, we place an eNB on its centroid. Thus, there are K_{macro} macro-cell eNBs and K_{micro} micro-cell eNBs in the service area.
- 2) Each UE $u_j \in \hat{U}$ then recalculates its group. Specifically, for each eNB $_i$, u_j calculates its *weighted distance* to the eNB as follows. If eNB $_i$ is a macro-cell eNB, then

$$d_W(u_j, \text{eNB}_i) = w_{macro} \cdot d(u_j, \text{eNB}_i);$$

otherwise,

$$d_W(u_j, \text{eNB}_i) = w_{micro} \cdot d(u_j, \text{eNB}_i),$$

where $d(u_j, \text{eNB}_i)$ denotes the Euclidian distance between u_j and eNB $_i$ and w_{macro} and w_{micro} are two weights used to control the size of each group. Then, UE u_j selects the eNB with the smallest $d_W(u_j, \text{eNB}_i)$ value and joins the eNB's group.

- 3) For each group, we compute its new centroid (of all UEs) and move the corresponding eNB to the centroid's position.
- 4) We repeat the above two steps until no eNB can be further moved.

By introducing two new weights w_{macro} and w_{micro} in step 2, all UEs in \hat{U} can be eventually partitioned into two-types of groups: *macro-cell groups* and *micro-cell groups*. As their name would suggest, we expect to use one macro-cell and micro-cell to cover all UEs in a macro-cell group and micro-cell group, respectively. To do so, we suggest setting $w_{macro} = 1/R_{macro}$ and $w_{micro} = 1/R_{micro}$. In addition, since the network operator can install eNBs on only the sites in \hat{E} , every time when the above approach calculates a new centroid to place an eNB, it has to check whether this centroid belongs to \hat{E} . If not, we select the nearest site in \hat{E} to be the new centroid.

We remark that stage 2 still uses the communication range R_{macro} and R_{micro} to help determine the locations of macro-cell and micro-cell eNBs. As mentioned earlier, the theoretical communication range of an eNB can be estimated by its transmission power in advance. However, a UE located inside the eNB's communication range does not guarantee that the eNB is able to serve it. Thus, we will do more precise deployment in the next stage, according to the result of stage 2.

4.3 Stage 3: Range Adjustment in Each Cell

Based on the flow diagram in Fig. 1, this stage iteratively examines whether every eNB has sufficient resource (that is, power and bandwidth) to serve all UEs in its cell, and then adjusts the cell range when necessary. Specifically, following the definitions in Section 3.3, we assume that each UE $u_j \in \hat{U}$ has the expected downlink traffic demand r_j^{DL} . Let $b_{i,j}^{DL}$ and $p_{i,j}$ be the downlink bandwidth and transmission power that an eNB $_i$ allocates to u_j . Then, according to the Shannon-Hartley theorem [32], given the signal-to-noise ratio (SNR) α , the achievable data rate of eNB $_i$ to u_j can be calculated by

$$r_{i,j}^{DL} = b_{i,j}^{DL} \cdot \lg(1 + \alpha) = b_{i,j}^{DL} \cdot \lg \left(1 + \frac{p_{i,j} \cdot H_{i,j}}{b_{i,j}^{DL} \Gamma N_0} \right), \quad (10)$$

and

$$H_{i,j} = \frac{|h_{i,j}|^2}{\Gamma N_0}, \quad (11)$$

where $h_{i,j}$ denotes the channel gain from eNB $_i$ to u_j , Γ is the SNR gap², and N_0 is the power spectral density of AWGN.

From Eq. (10), we can calculate the transmission power required by eNB $_i$ to let UE u_j have downlink data rate of $r_{i,j}^{DL}$ and bandwidth of $b_{i,j}^{DL}$:

$$p_{i,j} = \frac{b_{i,j}^{DL}}{H_{i,j}} \left(2^{r_{i,j}^{DL}/b_{i,j}^{DL}} - 1 \right). \quad (12)$$

Since UE u_j has the expected downlink traffic demand of r_j^{DL} , we can replace $r_{i,j}^{DL}$ by r_j^{DL} in Eq. (12). By combining Eqs. (11) and 12, we can derive that

$$p_{i,j} = \frac{b_{i,j}^{DL} \cdot \Gamma N_0}{|h_{i,j}|^2} \left(2^{r_j^{DL}/b_{i,j}^{DL}} - 1 \right). \quad (13)$$

2. The SNR gap Γ is usually a constant associated with a given bit-error-rate (BER) for a certain modulation and coding scheme. For example, the study of [33] shows that $\Gamma = -\ln(5\text{BER})/1.6$ when the uncoded MQAM (multi-level quadrature amplitude modulation) scheme is adopted.

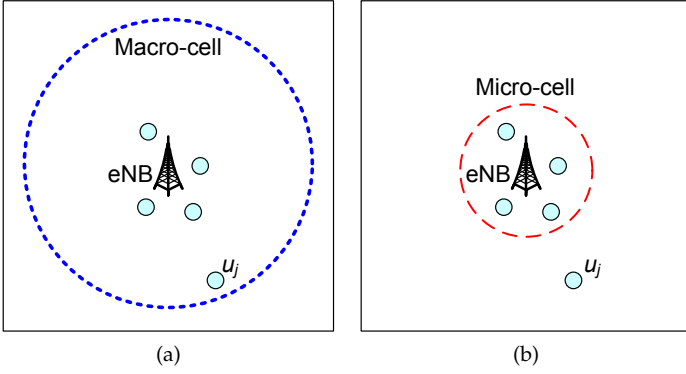


Fig. 3: An example of the second extension in stage 3: (a) the original macro-cell and (b) replacing the macro-cell with a micro-cell by discarding UE u_j .

Therefore, each eNB $_i$ can use Eq. (13) to determine whether it can support all UEs in its cell. Specifically, let $\hat{U}_i \subseteq \hat{U}$ denote the set of UEs in eNB $_i$'s cell (calculated by stage 2). Suppose that P_i and B_i^{DL} are the overall transmission power and downlink bandwidth of eNB $_i$, respectively. Obviously, when eNB $_i$ is a macro-cell eNB, then $P_i = P_{macro}$ and $B_i^{DL} = B_{macro}^{DL}$. On the other hand, $P_i = P_{micro}$ and $B_i^{DL} = B_{micro}^{DL}$ if eNB $_i$ is a micro-cell eNB. Then, eNB $_i$ can do the following check:

$$\sum_{u_j \in \hat{U}_i} p_{i,j} \leq P_i, \quad (14)$$

under the constraint of

$$\sum_{u_j \in \hat{U}_i} b_{i,j}^{DL} \leq B_i^{DL}. \quad (15)$$

Notice that $p_{i,j}$ and $b_{i,j}^{DL}$ are not fixed in the above calculation. Instead, they are computed by eNB $_i$ according to the expected downlink traffic demand r_j^{DL} . However, if eNB $_i$ cannot find a feasible solution of $p_{i,j}$ and $b_{i,j}^{DL}$ to satisfy Eqs. (14) and 15, it means that eNB $_i$ currently has no sufficient power or bandwidth resource to meet the downlink traffic demands of all its UEs. In this case, eNB $_i$ has to give up some UEs in the cell. Specifically, starting from the farthest UE, say, u_j , eNB $_i$ iteratively marks u_j as uncovered and removes the UE from its cell, until the above two equations become satisfied. Therefore, we can make sure that every eNB can support all UEs in its cell.

We remark that two extensions can help further improve stage 3. First, when a UE is marked as uncovered by its original eNB, the UE can check whether other nearby eNBs have sufficient power and bandwidth resource to serve it. If so, the UE can join the nearest one of such eNBs. Second, if a macro-cell eNB finds that it can use transmission power P_{micro} and downlink bandwidth B_{micro}^{DL} to serve all UEs in the current cell, then we can replace the eNB by a micro-cell eNB. This extension may occur when a macro-cell eNB discards some farther UEs and the residual UEs are close to it. Fig. 3 shows an example. When the macro-cell eNB discards the farthest UE u_j , then it can be replaced by a micro-cell eNB to serve the residual UEs.

4.4 Stage 4: Adding Pico-cells

After the range adjustment in stage 3, there could remain some UEs not covered by any large cell. These UEs are usually

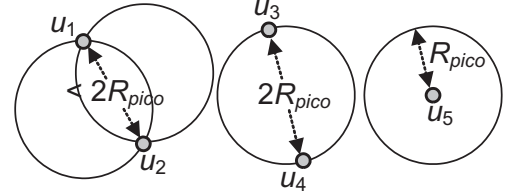


Fig. 4: Using the MGDC scheme to find the locations of pico-cells.

isolated from others, or locate near the boundary between two cells. Obviously, it is wasteful if we simply deploy macro-cells or micro-cells to cover such UEs, because each cell can only serve a small number of UEs. Therefore, we suggest using pico-cell eNBs to deal with this situation, as described in Fig. 1. Specifically, let $\hat{U}_R \subset \hat{U}$ denote the set of UEs not covered by any cell after stage 3. We then adopt the *modified geometric disk cover (MGDC) scheme* in [34] to find possible sites to deploy pico-cells, which involves the three rules:

- 1) If two UEs u_i and u_j in \hat{U}_R have a distance $d(u_i, u_j) < 2R_{pico}$, we deploy two pico-cells such that their circumferences intersect at u_i and u_j .
- 2) If two UEs u_i and u_j in \hat{U}_R have a distance $d(u_i, u_j) = 2R_{pico}$, we deploy one pico-cell such that its circumference passes both u_i and u_j .
- 3) If a UE $u_k \in \hat{U}_R$ is isolated, which means that its distance to the closest UE is larger than $2R_{pico}$, we deploy a pico-cell whose center is on u_k .

Fig. 4 gives three examples. Since we have to check each pair of UEs in \hat{U}_R , the maximum number of pico-cells found by the MGDC scheme will be $2C_2^{|\hat{U}_R|}$, where $C_2^{|\hat{U}_R|} = \frac{|\hat{U}_R|!}{2!(|\hat{U}_R|-2)!}$ is the combination of selecting two UEs from the set \hat{U}_R . In practice, we require at most $|\hat{U}_R|$ pico-cells to cover these UEs. Therefore, among all pico-cells found by the MGDC scheme, we select the pico-cell whose center belongs to \hat{E} (that is, the network operator can deploy a pico-cell eNB on that location) and it can cover the maximum number of UEs in \hat{U}_R . Then, we use the scheme in Section 4.3 again to determine the UEs that can be served by the corresponding pico-cell eNB (to satisfy Eqs. (14) and 15 where $P_i = P_{pico}$ and $B_i^{DL} = B_{pico}^{DL}$). The above iteration is repeated until all UEs in \hat{U}_R are served by pico-cell eNBs.

4.5 Rationale of the eNB Deployment Strategy

Given the transmission power of an eNB, we can easily derive its theoretical communication range. Besides, some eNB manufacturers also give both the parameters of transmission power and communication range in their products. Therefore, our eNB deployment strategy takes advantage of these two parameters and can be roughly divided into two parts, as shown in Fig. 1. In the first part (that is, stages 1 and 2), we seek to determine the locations of eNBs from a geometric perspective so as to provide the preliminary network deployment. Specifically, our objective is to identify where most of UEs congregate so that we can effectively employ large cells such as macro-cells and micro-cells to cover them. However, a UE that can be covered by an eNB does not imply that the eNB can provide service to meet the traffic demand of that UE. Therefore, the second part of our strategy (that is, stages 3 and 4) attempts to determine the actual service range of each eNB

from a resource's perspective. In particular, we carefully check if every eNB has sufficient amount of power and bandwidth to support all UEs in its cell, and adjust their cell range if necessary. Then, we would add small pico-cells to strengthen the network deployment.

For the first part, K -means is a popular solution to group UEs according to their relative geographic locations. However, the traditional K -means approach cannot be directly applied to our EDMC problem because of two reasons: 1) The K -means approach requires the knowledge of K value in advance. 2) The K -means approach does not take the size of macro-cells and micro-cells (that is, R_{macro} and R_{micro}) into consideration. To solve these two problems, we modify the AHC scheme in stage 1 to estimate the number of macro-cells and micro-cells required to cover all UEs (based on the R_{macro} and R_{micro} values). Then, in stage 2, we introduce two weights w_{macro} and w_{micro} to the K -means approach, so that UEs can be partitioned into multiple groups such that the size of each group could be constrained by either a macro-cell or micro-cell in substance. This is realized by setting $w_{macro} = 1/R_{macro}$ and $w_{micro} = 1/R_{micro}$ (that is, the reciprocal of the communication range of an eNB).

It is noteworthy that one may argue that the AHC scheme has already provided a clustering result to deploy macro-cells and micro-cells, which makes the weighted K -means approach in stage 2 become redundant. However, stage 2 is necessary to our eNB deployment strategy due to the following reason: The AHC scheme iteratively combines two clusters according to their inter-cluster distance. Unlike the weighted K -means approach, it does not take the congregation degree of UEs into account. Therefore, a larger macro-cell could cover just few UEs (if they are sparsely scattered) whereas a smaller micro-cell may have to cover a lot of UEs. Using the weighted K -means approach can alleviate the above situation by balancing UEs among different cells. Through the simulations in Section 6, we will also show that using the weighted K -means approach in stage 2 can significantly outperforms the case of using only the AHC scheme.

For the second part, we use the expected downlink traffic demand r_j^{DL} of each UE u_j in stage 3 to estimate the amount of downlink bandwidth and power that its eNB has to allocate. However, the overall allocation of bandwidth and power cannot exceed the eNB's thresholds B_{macro}^{DL} (or B_{micro}^{DL}) and P_{macro} (or P_{micro}). In case an eNB does not have sufficient resource to satisfy the downlink traffic demands of all its UEs, the eNB iteratively removes the farthest UE until the residual UEs can be served. Since there is a high possibility that farther UEs will encounter worse channel quality (and lower SNR values), removing such UEs can help improve the network throughput in a cell. We also discuss two extensions in Section 4.3 to adaptively expand or shrink cell range so as to reduce the system cost. However, if there are still some UEs not covered by any cell, we finally add pico-cells in stage 4 to serve them. Here, because a pico-cell has quite smaller communication range (referring to Table 1), we only use them to strength the network deployment by serving the UEs that are isolated from others or cannot be covered by large cells. Therefore, we can further save the system cost since pico-cell eNBs have a lower price and maintenance cost as compared with large-cell eNBs.

5 DISCUSSIONS ON THE ENB DEPLOYMENT STRATEGY

In this section, we investigate several research issues arisen in our eNB deployment strategy, including the fluctuations in UE density, impact of uplink transmission, and cell interference.

5.1 Fluctuations in UE Density

The EDMC problem considers that the locations of UEs are deterministic and known in advance. In practice, the UE density will fluctuate over different times. For example, a downtown office area usually contains many UEs in work-days but may become almost empty during weekends. Such fluctuations could be regular and even predictable. To accommodate our eNB deployment strategy to the above situation, we suggest that the network operator should gather statistics of UE distributions during different periods on each day in a week (for example, morning, afternoon, and night time of one day). Let \hat{U}_k denote the set of UEs observed in period k and $\hat{U} = \bigcup_{\forall k} \hat{U}_k$. Based on the information from \hat{U} , the network operator can plan to deploy all necessary eNBs in the service area in order to react to the regular change of UE density. Specifically, When the UE density or traffic demands change substantially, the network operator can employ our eNB deployment strategy to calculate the subset of eNBs that should be kept operating to provide service. Then, other unnecessary eNBs can be temporarily switched off to reduce the amount of energy consumption.

Sometimes, a service area may ordinarily contain few UEs but is crowded with a large number of UEs in short term due to special activities (for example, a singing concert). In this case, it is not economic for the network operator to deploy a lot of eNBs in advance because the UE density will suddenly decrease once the activity finishes. To deal with such situations, the network operator can use the set of UEs appearing in the service area in ordinary time to calculate the locations to deploy *backbone eNBs*. Then, when many exterior UEs come into the service area, the network operator may adaptively add 'maneuverable' eNBs such as *mobile relay stations* [35], [36] to serve these UEs. In this way, the network operator can deal with the case when the UE density changes drastically and irregularly, because some eNBs could be dynamically moved to different locations to support various communication missions.

The above two scenarios also demonstrate the benefit of using LTE HetNets. In particular, once the eNB deployment for an LTE HetNet is determined, the network operator can choose to switch eNBs on/off to save energy or dispatch maneuverable eNBs to meet high traffic demands. Therefore, it not only accommodates an LTE HetNet to the changed environment (for example, diverse UE density) but also helps decrease the cost of maintenance and operation.

5.2 Impact of Uplink Transmission

In stages 3 and 4 of our eNB deployment strategy, we employ the transmission power of an eNB (that is, P_{macro} , P_{micro} , and P_{pico}) to determine whether the eNB can support the traffic demands of all UEs in its cell. However, the above determination is from a 'downlink' perspective. Due to the power limitation of UEs, it may not guarantee that each UE can successfully transmit the uplink data to its eNB. To solve this problem, we revise Eq. (13) to check if every eNB can

receive the uplink data from all of its UEs. Specifically, let P_{UE} denote the typical transmission power of UEs. From Eq. (13), we can derive that

$$b_{i,j}^{UL} \cdot (2^{r_j^{UL}/b_{i,j}^{UL}} - 1) = \frac{P_{UE} \cdot |h_{j,i}|^2}{\Gamma N_0} \quad (16)$$

Here, $b_{i,j}^{UL}$ is the bandwidth that eNB $_i$ allocates for UE u_j to transmit its uplink data, r_j^{UL} is expected uplink traffic demand of u_j , and $h_{j,i}$ is the channel gain from u_j to eNB $_i$. In Eq. (16), we are given the parameters of P_{UE} and r_j^{UL} in advance. Besides, $h_{j,i}$, Γ , and N_0 are known environmental parameters. Therefore, we can calculate the necessary uplink bandwidth $b_{i,j}^{UL}$ that eNB $_i$ should reserve for u_j . Then, for each eNB $_i$, we check whether

$$\sum_{u_j \in \hat{U}_i} b_{i,j}^{UL} \leq B_i^{UL}, \quad (17)$$

where $B_i^{UL} \in \{B_{macro}^{UL}, B_{micro}^{UL}, B_{pico}^{UL}\}$ is the total uplink bandwidth of an eNB (depending on its type) and \hat{U}_i is the set of UEs served by eNB $_i$. If Eq. (17) is violated, which means that some UEs may fail to send their uplink data, eNB $_i$ then iteratively removes the farthest UE in its cell, until Eq. (17) becomes satisfied.

5.3 Cell Interference

In Section 3.1, we mention that the communication range of an eNB can be estimated by its transmission power. It has been pointed out in [37] that such estimation highly depends on the path-loss fading. Therefore, given the transmission power of an eNB, we can employ Eqs. (1) and 2 to calculate its corresponding communication range, without caring about which component carriers assigned to that eNB. However, once the locations of eNBs are determined, the assignment of component carriers becomes important. In particular, if two adjacent eNBs are assigned with the similar component carriers, they may cause interference between each other. Fortunately, LTE introduces the technology of ICIC (*inter-cell interference coordination*) and eICIC (*enhanced ICIC*) to deal with the above interference problem. ICIC allows eNBs to negotiate the usage of resource blocks through their X2 interfaces. Therefore, UEs near the cell edges are allocated with different resource blocks to avoid interference. On the other hand, eICIC is developed for LTE HetNets, which employs different negotiation strategies for different types of eNBs. In addition, eICIC proposes the concept of *almost blank subframe (ABS)* to alleviate the interference to a small cell (such as pico-cells) from a large macro-cell. Due to the page limitation, we leave the details of both ICIC and eICIC in [38].

6 EXPERIMENTAL RESULTS

In this section, we measure the performance of our eNB deployment strategy by using MATLAB, which provides modules to simulate LTE channels (for example, multipath fading). Table 2 lists our simulation parameters for eNBs. The typical transmission power of UEs P_{UE} is set to 27 dBm (around 500 mW). The expected uplink and downlink traffic demands of UEs are randomly picked from $r_j^{UL} \in [0, 0.3]$ Mbps and $r_j^{DL} \in [0.1, 1.0]$ Mbps, respectively. Besides, we consider four scenarios to model the distribution of UEs:

- **Small-group scenario:** There are 300 UEs placed in a 12 km \times 16 km service area. Most UEs congregate in the

TABLE 2: Simulation parameters for LTE eNBs.

parameters	macro-cell	micro-cell	pico-cell
cell size	3 km	1 km	0.1 km
power	46 dBm (40 W)	33 dBm (2 W)	24 dBm (0.25 W)
bandwidth*	100 MHz	100 MHz	30 MHz
cost [25]	397,800 Euros	42,200 Euros	12,400 Euros
path loss	Eq. (1)	Eq. (2)	Eq. (2)
slow fading	$\mu = 0, \sigma = 10$ dB	$\mu = 0, \sigma = 6$ dB	$\mu = 0, \sigma = 6$ dB
common parameters	AWGN power density (N_0): -174 dBm/Hz Bit error rate (BER): 10^{-6} SNR gap (Γ): 7.6288		

*The ratio of uplink to downlink bandwidth is 1:4.

middle part of the service area, as shown in Fig. 5(a). In this scenario, the network operator can deploy eNBs at any locations inside the service area.

- **Large-group scenario:** We consider a 20 km \times 20 km service area over which 600 UEs are scattered following the normal distribution, as illustrated in Fig. 5(b). Similar to the above scenario, the network operator can freely deploy eNBs in the service area.
- **Multi-group scenario:** Totally 1,800 UEs are placed in a 30 km \times 35 km service area and they can be roughly divided into five groups, as Fig. 5(c) presents. Again, the network operator can choose any locations to deploy eNBs.
- **Downtown scenario:** We take a part of the downtown area in Kaohsiung City, Taiwan to be the service area, which is a square region whose wide is 18 km, as shown in Fig. 5(d). In this scenario, the network operator is allowed to deploy eNBs only along streets (that is, \hat{E} contains all street subregions).

We compare our proposed eNB deployment strategy with three methods:

- **Macro-cell deployment (MCD) method:** Like 2G and 3G systems, this method deploys only macro-cell eNBs. We employ the rules in stage 3 to check whether every macro-cell eNB can serve all UEs in its cell and add extra macro-cells to the service area when necessary. The MCD method is used as a baseline to observe the benefit and flexibility of using LTE HetNets.
- **AHC two-type-cell deployment (ATD) method:** We adopt the modified AHC scheme in stage 1 to cluster UEs into macro-cell and micro-cell groups. For each group of UEs, we deploy the corresponding type of eNB to provide service. Then, after shrinking the cell range of eNBs (by stage 3), we add micro-cells to cover those unserved UEs.
- **Traditional K -means deployment (TKD) method:** It is similar to our eNB deployment strategy, but in stage 3 we use the traditional K -means approach to help deploy eNBs. In addition, this method does not employ the two extensions proposed in stage 3.

Each experiment contains 100 simulations, where in each simulation we randomly generate the expected traffic demands of UEs (that is, r_j^{UL} and r_j^{DL}) to observe their effect. According to the locations of UEs (defined in the four scenarios) and their demands, each deployment method then determines where to install eNBs and calculates the amount of their power consumption. We then take the average of these 100 simulation results in each experiment.

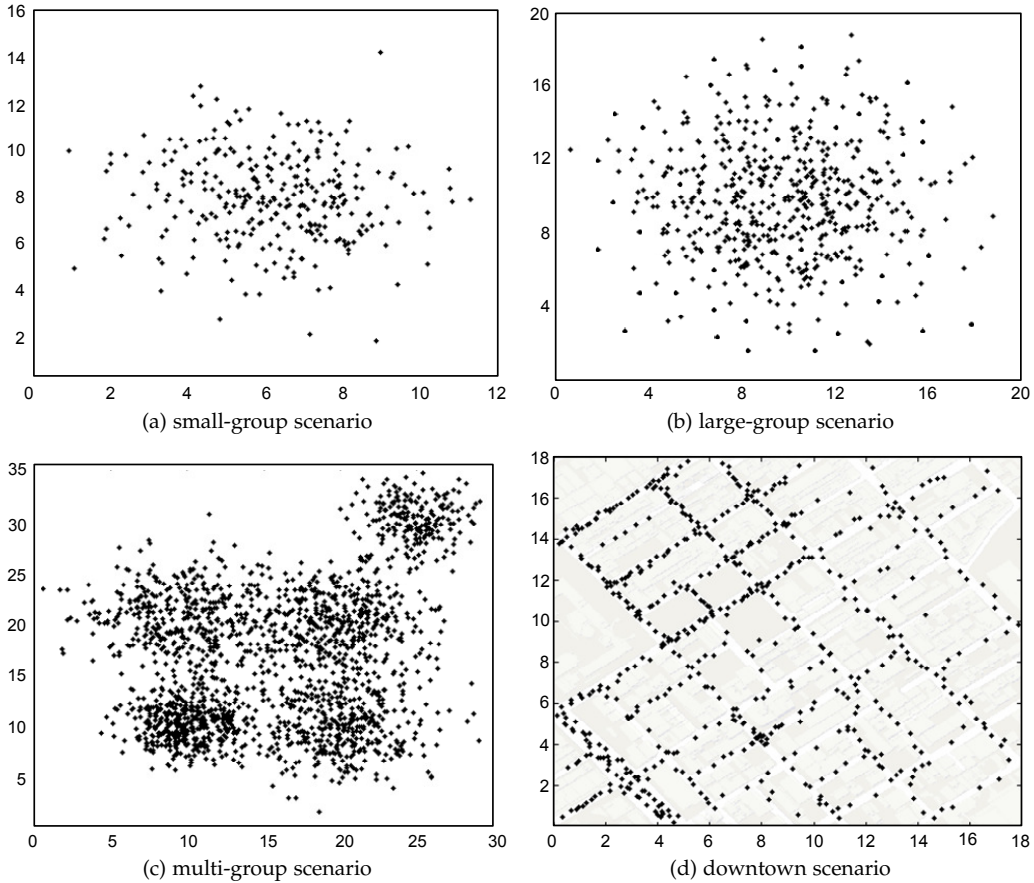


Fig. 5: Four scenarios to model the distribution of UEs.

6.1 System Cost

Using the four scenarios in Fig. 5, we first evaluate the system costs spent by the MCD, ATD, and TKD methods and our eNB deployment strategy, as shown in Fig. 6. Apparently, the system cost increases as the number of UEs grows because each eNB has limited power and bandwidth resource to serve them. The MCD method considers only macro-cells, so it always results in the highest system cost. On the contrary, by deploying different types of eNBs in the service area, other three methods can greatly reduce the overall system cost. From Fig. 6, we can observe that the ATD and TKD methods use the same number of macro-cell eNBs because they both employ the modified AHC scheme to calculate the required number of macro-cell eNBs (that is, K_{macro}). The ATD method needs slightly more micro-cell eNBs than the TKD method since it employs extra micro-cell eNBs to cover those unserved UEs after shrinking the cell range of macro-cell eNBs. However, the TKD method just uses the traditional K -means approach to cluster UEs, which does not consider the difference between macro-cells and micro-cells. Thus, it would require more pico-cells to cover those unserved UEs and thus increases the system cost. On the other hand, by adopting the two extensions proposed in stage 3, our eNB deployment strategy can further reduce macro-cells deployed in the service area. In this case, it suggests using smaller micro-cells and pico-cells to help cover the service area in order to save the overall system cost. On average, our eNB deployment strategy can save 48.07%, 21.59%, and 22.49% of the system cost compared with the MCD, ATD, and TKD methods, respectively, in the four scenarios of UE distribution.

Both the large-group and downtown scenarios have the

same number of users (that is, 600 UEs). However, when comparing Fig. 6(b) with Fig. 6(d), we can observe that all deployment methods require more system costs in the downtown scenario than that in the large-group scenario. There are two reasons to cause such phenomena. First, the large-group scenario lets UEs be scattered over the service area by using the normal distribution. In this case, we can deploy macro-cells near the central part of the area to cover a larger number of UEs. On the other hand, UEs arbitrarily appear along the streets in the downtown scenario, so it is not easy to deploy just few macro-cells to cover most of UEs. Second, the network operator can freely deploy eNBs in the large-group scenario but is allowed to install eNBs only on the street subregions in the downtown scenario. The constraint of \hat{E} in the downtown scenario would force the network operator to use more eNBs to serve UEs as it cannot install eNBs on those 'good' locations not in \hat{E} .

Recall that we have discussed the two possible solutions to the problem of fluctuations in UE density in Section 5.1. Suppose that the network operator knows that the distribution of UEs will alternate between the small-group scenario and the large-group scenario in Fig. 5. Then, we can take the union of both scenarios to calculate the locations to install all necessary eNBs. When the distribution of UEs change from one scenario to another scenario, the network operator can adaptively switch off unnecessary eNBs to react to the distribution change of UEs. On the other hand, suppose that the distribution of UEs in a service area follows the large-group scenario in ordinary time but may evolve to the multi-group scenario due to some special activity. In this case, the network

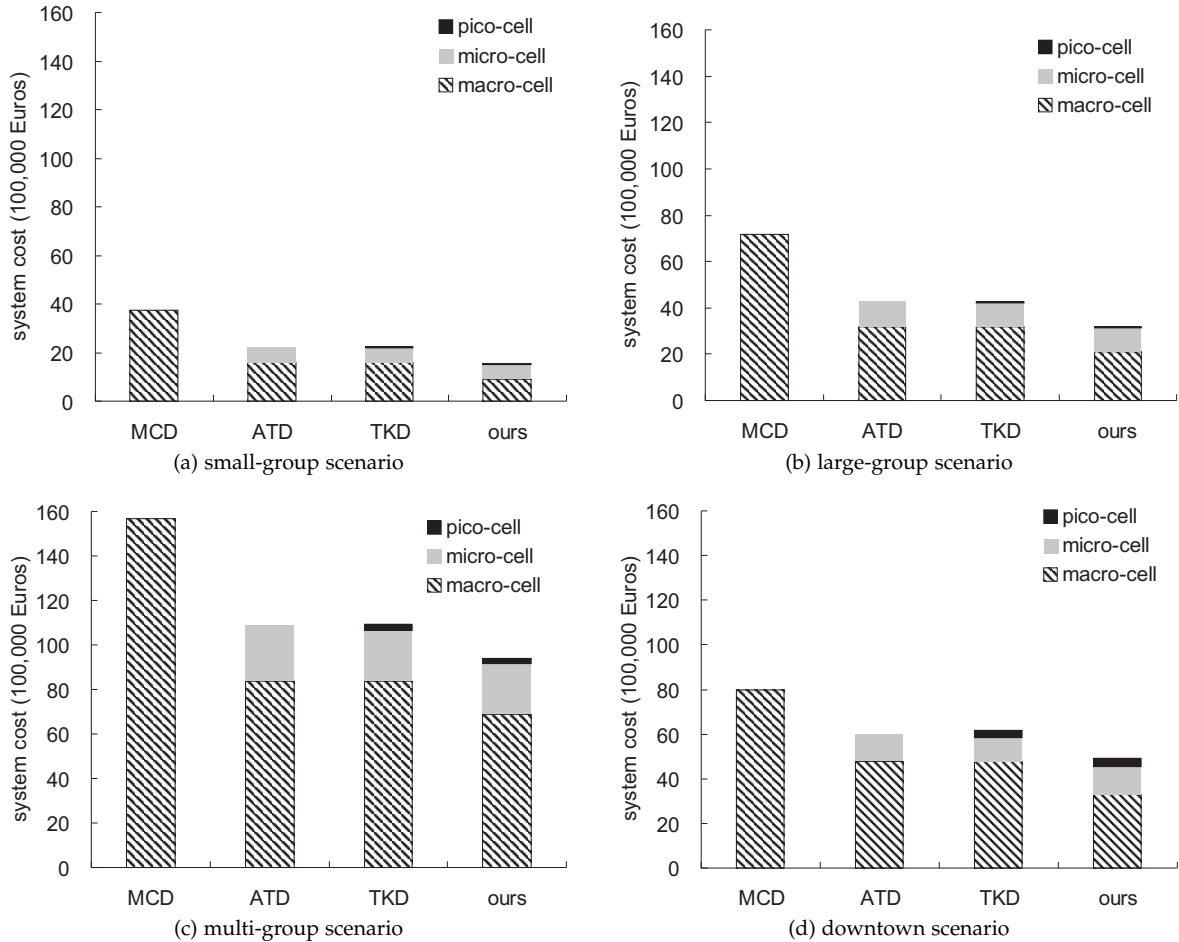


Fig. 6: Comparison on the system costs required by different deployment methods.

operator can first use the large-group scenario to deploy the backbone network. Then, we can use the multi-group scenario to calculate additional mobile relay stations required to serve the exterior UEs crowding into the service area.

We remark that the expected traffic demands of UEs are randomly generated in the experiment. For the MCD method, changing traffic demands would affect the number of macro-cells deployed in the service area. However, it has less effect on the macro-cells deployed by other three methods. The reason is that these methods can instead employ smaller micro-cells or pico-cells to deal with the change of traffic demands. This phenomenon shows the benefit of using LTE HetNets, where the network operator can dynamically add low-cost small-cells to satisfy a small increase of traffic demands from UEs.

6.2 Power Consumption

We then measure the amount of power consumed by all eNBs deployed in different methods, which can be also used to evaluate the *eNB maintenance cost* after the network deployment. In this experiment, the average downlink traffic demand of UEs is ranged from 0.1 Mbps to 1 Mbps. Fig. 7(a) shows the simulation result in the small-group scenario. Obviously, when the traffic demand grows, each eNB has to emit larger power to improve the downlink channel quality. The MCD method always lets eNBs consume the largest power because some macro-cell eNBs have to take care of those 'sparse' UEs far away from others. Since these UEs usually appear near the boundary of macro-cells, the eNBs have to transmit in larger power to

improve their channel quality. On the other hand, the TKD method can reduce the power consumption compared with the ATD method. Although the ATD method has a slightly cheaper system cost than the TKD method (referring to Fig. 6), it does not place macro-cells and micro-cells in 'suitable' locations. Specifically, the ATD method tries to group UEs into clusters which can be fitted into one macro-cell or micro-cell. In this case, it may place some cells to cover those sparse UEs (similar to the MCD method). On the contrary, the TKD method uses pico-cells to cover such UEs so that macro-cells and micro-cells can be placed on the regions where most UEs congregate. That is why the TKD method has less power consumption than the ATD method. By adaptively adjusting the locations and coverage of cells, our eNB deployment strategy helps eNBs consume the least amount of transmission power to satisfy the traffic demands of all UEs. In other words, it can significantly save the maintenance cost after deploying eNBs.

Fig. 7(b) presents the ratios of power consumed by macro-cell, micro-cell, and pico-cell eNBs in the small-group scenario. The ratio of power consumed by macro-cell eNBs in the MCD method is 100%. For both the ATD and TKD methods, macro-cell eNBs contribute more than 96% of total power consumption. This result points out that both methods do not well utilize the benefit of LTE HetNets. On the contrary, the ratio of power consumed by micro-cell and pico-cell eNBs in our eNB deployment strategy is around 20.57%. This implicitly means that our eNB deployment strategy can deal out the traffic loads of macro-cell eNBs to the nearby small-cell eNBs.

Figs. 8, 9, and 10 present the power consumption of all

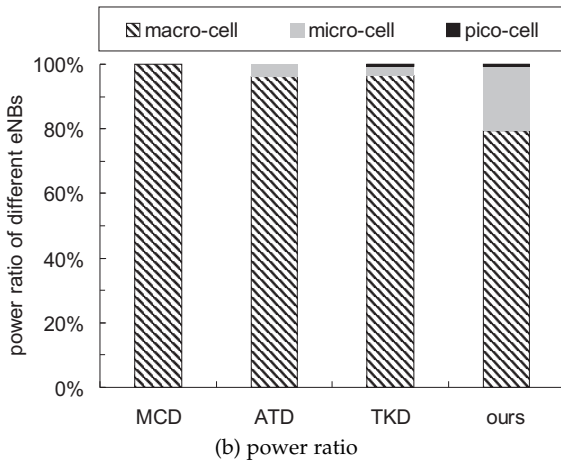
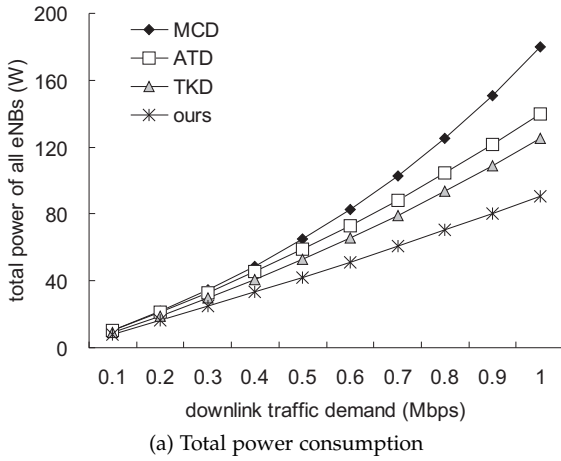


Fig. 7: Total power consumption of all eNBs and the ratios of power consumed by different types of eNBs in the small-group scenario.

eNBs and the ratios of power spent by different types of eNBs in the large-group, multi-group, and downtown scenarios, respectively. These results are similar to Fig. 7, where our eNB deployment strategy always allows eNBs to emit less power to satisfy the growing demand of UEs. Besides, the ratio of power consumed by macro-cell eNBs in our eNB deployment strategy is around 77.05%, 80.03%, and 73.53% in the large-group, multi-group, and downtown scenarios, respectively, which is significantly lower than that in the other three methods. Interestingly, in the downtown scenario, the pico-cell eNBs contribute more power consumption by the TKD method and our eNB deployment strategy, as shown in Fig. 10(b). Because UEs are scattered over streets in this scenario, both methods prefer using more pico-cells to serve sparse UEs, thereby increasing the corresponding power ratio.

6.3 Load Balance

Finally, we observe the standard deviation of the amount of power consumption of all macro-cell eNBs, which can be used to estimate their *load-balancing degree*. In particular, a smaller standard deviation indicates that most of macro-cell eNBs can emit the similar amount of transmission power, so their traffic loads are more balanced. By varying the downlink traffic demands from UEs, Fig. 11 shows the experimental results. Obviously, because the MCD method considers homogeneous macro-cell eNBs, it always results in the largest standard deviation in different scenarios. On the other hand, the ATD method divides UEs into groups where the diameter of each

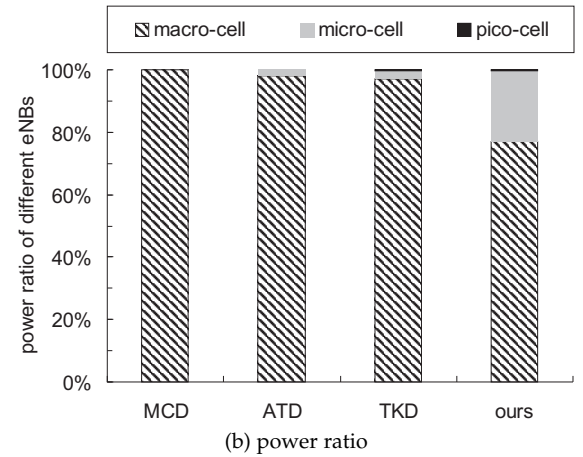
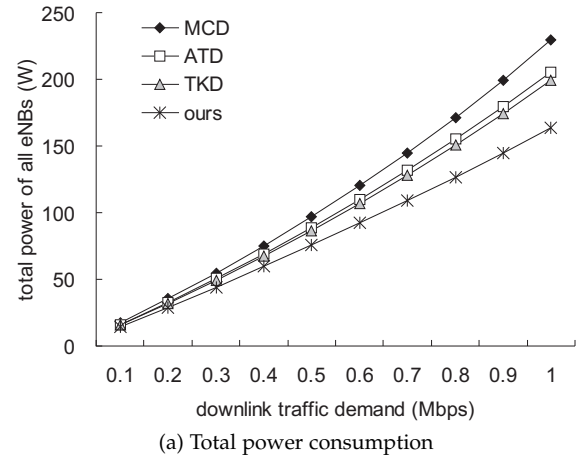
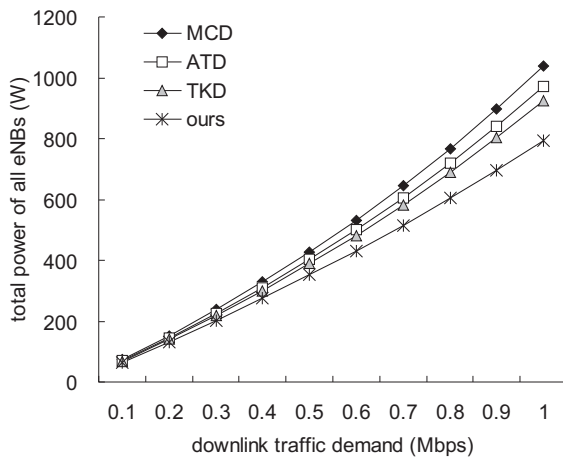


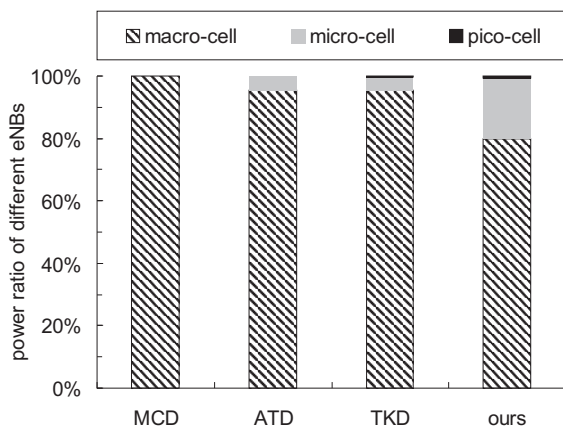
Fig. 8: Total power consumption of all eNBs and the ratios of power consumed by different types of eNBs in the large-group scenario.

group is no larger than R_{macro} or R_{micro} . In this case, some macro-cells may cover only few UEs so as to increase the standard deviation of power consumption. Both the TKD method and our eNB deployment strategy employ the concept of K -means to group UEs based on their geographic relationships. Therefore, they seek to deploy macro-cell eNBs to cover similar number of UEs and thereby reduce the standard deviation of power consumption.

From Fig. 11, we can observe that the standard deviation of power consumption increases as the downlink traffic demand grows. Such phenomena become more significant in the small-group and multi-group scenarios, as shown in Fig. 11(a) and (c). The reason is that UEs congregate in certain parts of the service area in these two scenarios. In particular, most of UEs appear in the core of the service area in the small-group scenario (referring to Fig. 5(a)), while the multi-group scenario obviously contains five groups of UEs (referring to Fig. 5(c)). Due to such uneven distributions of UEs, the macro-cells deployed in the subregions where UEs congregate will cover a large number of UEs, while others may serve only a small number of UEs. Thus, the standard deviation of power consumption substantially increases, especially when the traffic demands grow. In contrast with the above two scenarios, UEs are distributed over the service area more uniformly in both the large-group and downtown scenarios (referring to Fig. 5(b) and (d)). Therefore, the standard deviation of power consumption can be reduced in Fig. 11(b) and (d). In these two cases, our eNB deployment strategy can group UEs more



(a) Total power consumption



(b) power ratio

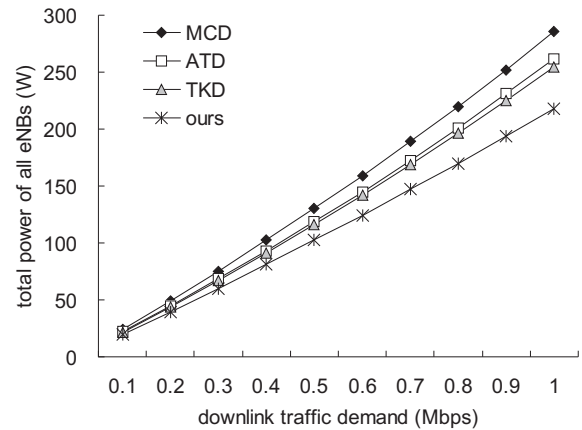
Fig. 9: Total power consumption of all eNBs and the ratios of power consumed by different types of eNBs in the multi-group scenario.

efficiently through the weighted K -means approach, thereby resulting in lower standard deviation of power consumption as compared with the TKD method.

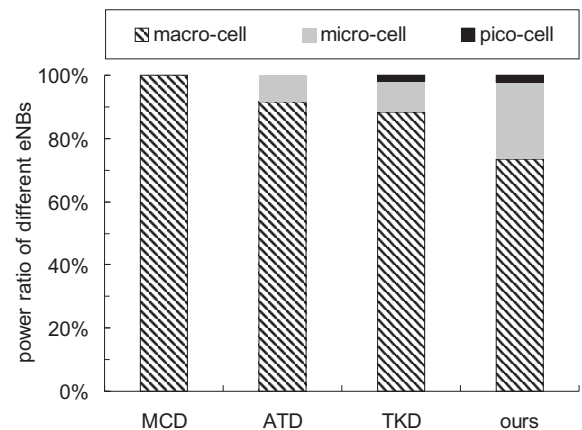
7 CONCLUSION AND FUTURE WORK

By allowing various eNBs to cooperate in a service area, LTE HetNets become more flexible than conventional 2G/3G homogeneous networks. This paper thus formulates an NP-hard EDMC problem with the objective of minimizing the system cost to deploy an LTE HetNet such that user demands are satisfied. An efficient eNB deployment strategy is proposed from the perspectives of both geometry and resource. In particular, based on the communication range of eNBs, the deployment strategy first employs the modified AHC scheme and the weighted K -means approach to cluster UEs. Then, under the power and bandwidth constraints of each eNB, it adaptively adjusts the cell range to meet the traffic demands of all serving UEs and tactically adds pico-cells when necessary. We also extend our eNB deployment strategy by considering the fluctuations in UE density, impact of uplink transmission, and cell interference. Through the four scenarios to model the distribution of UEs, extensive simulation results show that our eNB deployment strategy can save the system cost, reduce the power consumption of eNBs, and balance the traffic loads of macro-cells.

In this paper, we aim at the *initial construction* of an LTE system by deploying different types of eNBs in a service area.



(a) Total power consumption



(b) power ratio

Fig. 10: Total power consumption of all eNBs and the ratios of power consumed by different types of eNBs in the downtown scenario.

However, in some cases, macro-cell eNBs may have already existed in the service area for operating and it is difficult to 'redeploy' additional macro-cell eNBs due to some reasons (for example, site acquisition is too expensive). Therefore, it deserves further investigation of how to add only small-cell eNBs in an existing LTE network to satisfy user demands while minimizing both the cost and interference. Alternatively, we can adaptively adjust the transmission power of existing macro-cell eNBs to accommodate the network to the changed user demands.

REFERENCES

- [1] ITU Radiocommunication Sector, "Background on IMT-Advanced," Technical Report, IMT-ADV/1, 2008.
- [2] D. Astely, E. Dahlman, A. Furuskar, Y. Jading, M. Lindstrom, and S. Parkvall, "LTE: the evolution of mobile broadband," *IEEE Comm. Magazine*, vol. 47, no. 4, pp. 44–51, 2009.
- [3] S. Barbera, P.H. Michaelsen, M. Saily, and K. Pedersen, "Mobility performance of LTE co-channel deployment of macro and pico cells," *Proc. IEEE Wireless Comm. and Networking Conf.*, 2012, pp. 2863–2868.
- [4] A. Khandekar, N. Bhushan, J. Tingfang, and V. Vanghi, "LTE-Advanced: heterogeneous networks," *European Wireless Conf.*, 2010, pp. 978–982.
- [5] A. Damnjanovic, J. Montojo, Y. Wei, T. Ji, T. Luo, M. Vajapeyam, T. Yoo, O. Song, and D. Malladi, "A survey on 3GPP heterogeneous networks," *IEEE Wireless Comm.*, vol. 18, no. 3, pp. 10–21, 2011.
- [6] Fujitsu, "High-capacity indoor wireless solutions: picocell or femto-cell?" <http://www.fujitsu.com/downloads/TEL/fnc/whitepapers/High-Capacity-Indoor-Wireless.pdf>, 2014.
- [7] C. Lee and H. Kang, "Cell planning with capacity expansion in mobile communications: a tabu search approach," *IEEE Trans. Vehicular Technology*, vol. 49, no. 5, pp. 1678–1691, 2000.

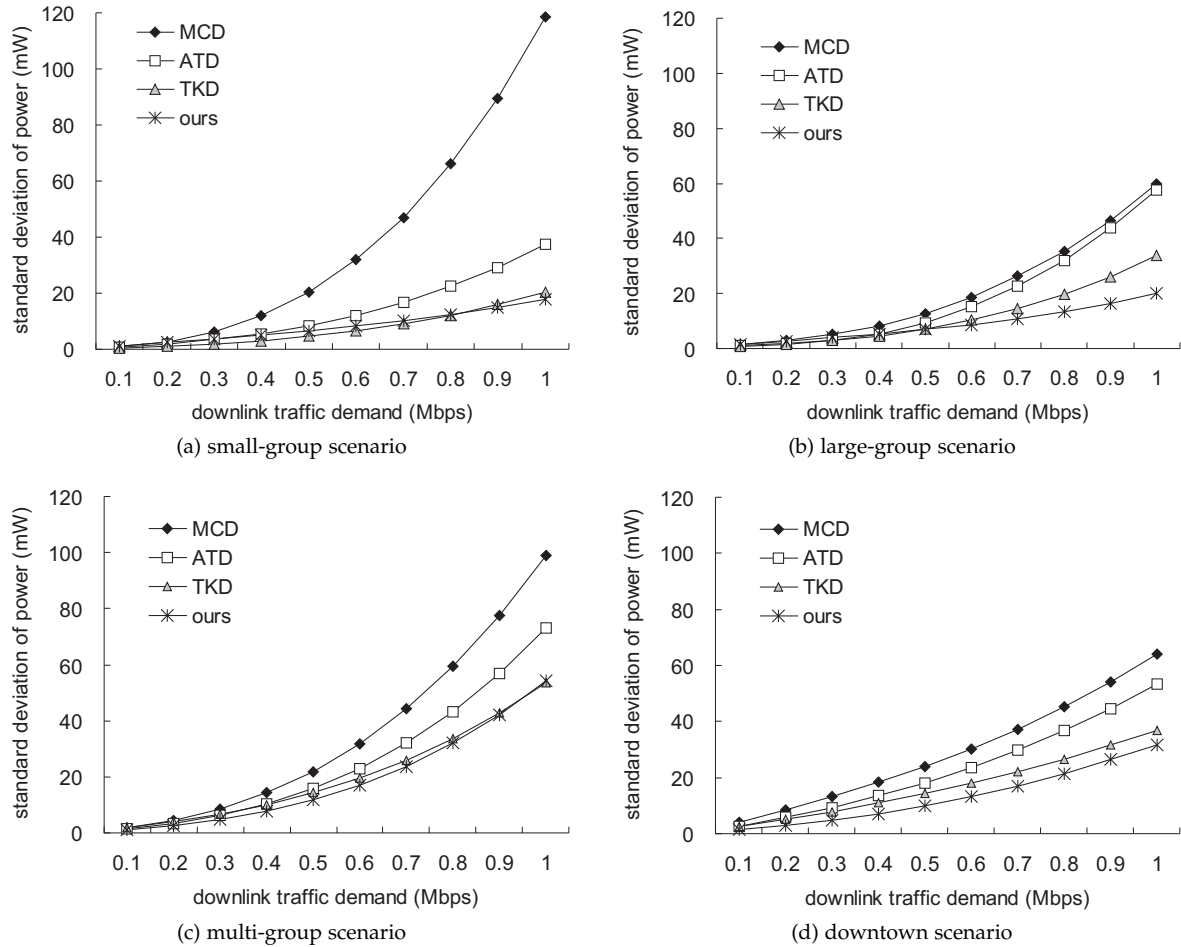


Fig. 11: Comparison on the standard deviation of the amount of power consumed by macro-cell eNBs in different deployment methods.

- [8] S. Hurley, "Planning effective cellular mobile radio networks," *IEEE Trans. Vehicular Technology*, vol. 51, no. 2, pp. 243–253, 2002.
- [9] N. Weicker, G. Szabo, K. Weicker, and P. Widmayer, "Evolutionary multiobjective optimization for base station transmitter placement with frequency assignment," *IEEE Trans. Evolutionary Computation*, vol. 7, no. 2, pp. 189–203, 2003.
- [10] J. Kalvenes, J. Kennington, and E. Olinick, "Hierarchical cellular network design with channel allocation," *European J. Operational Research*, vol. 160, no. 1, pp. 3–18, 2005.
- [11] E. Amaldi, A. Capone, and F. Malucelli, "Planning UMTS base station location: optimization models with power control and algorithms," *IEEE Trans. Wireless Comm.*, vol. 2, no. 5, pp. 939–952, 2003.
- [12] J. Yang, M. Aydin, J. Zhang, and C. Maple, "UMTS base station location planning: a mathematical model and heuristic optimisation algorithms," *IET Comm.*, vol. 1, no. 5, pp. 1007–1014, 2007.
- [13] H.Y. Zhang, Y.G. Xi, and H.Y. Gu, "A rolling window optimization method for large-scale WCDMA base stations planning problem," *European J. Operational Research*, vol. 183, no. 1, pp. 370–383, 2007.
- [14] E. Amaldi and A. Capone, "Radio planning and coverage optimization of 3G cellular networks," *Wireless Networks*, vol. 14, no. 4, pp. 435–447, 2008.
- [15] C.K. Ting, C.N. Lee, H.C. Chang, and J.S. Wu, "Wireless heterogeneous transmitter placement using multiobjective variable-length genetic algorithm," *IEEE Trans. Systems, Man, and Cybernetics, Part B: Cybernetics*, vol. 39, no. 4, pp. 945–958, 2009.
- [16] S. Wang, W. Zhao, and C. Wang, "Budgeted cell planning for cellular networks with small cells," *IEEE Trans. Vehicular Technology*, 2015.
- [17] A. Simonsson, B. Hagerman, J. Chistoffersson, L. Klockar, C. Koutsimanis, and P. Cosimini, "LTE downlink inter-cell interference assessment in an existing GSM metropolitan deployment," *Proc. IEEE Vehicular Technology Conf.*, 2010, pp. 1–5.
- [18] Y. Wu, D. Zhang, H. Jiang, and Y. Wu, "A novel spectrum arrangement scheme for femto cell deployment in LTE macro cells," *Proc. IEEE Int'l Symp. Personal, Indoor and Mobile Radio Comm.*, 2009, pp. 6–11.
- [19] P. Lin, J. Zhang, Y. Chen, and Q. Zhang, "Macro-femto heterogeneous network deployment and management: from business models to technical solutions," *IEEE Wireless Comm.*, vol. 18, no. 3, pp. 64–70, 2011.
- [20] S. Kaneko, T. Matsunaka, and Y. Kishi, "A cell-planning model for HetNet with CRE and TDM-ICIC in LTE-Advanced," *Proc. IEEE Vehicular Technology Conf.*, 2012, pp. 1–5.
- [21] X. Gelabert, G. Zhou, and P. Legg, "Mobility performance and suitability of macro cell power-off in LTE dense small cell HetNets," *Proc. IEEE Int'l Workshop on Computer Aided Modeling and Design of Comm. Links and Networks*, 2013, pp. 99–103.
- [22] W. Zhao and S. Wang, "Cell planning for heterogeneous cellular networks," *Proc. IEEE Wireless Comm. and Networking Conf.*, 2013, pp. 1032–1037.
- [23] W. Zhao, S. Wang, C. Wang, and X. Wu, "Cell planning for heterogeneous networks: an approximation algorithm," *proc. IEEE INFOCOM*, 2014, pp. 1087–1095.
- [24] E. Dahlman, S. Parkvall, and J. Skold, *4G: LTE/LTE-Advanced for Mobile Broadband*, Elsevier, 2013.
- [25] M. Döttling, W. Mohr, and A. Osseiran, *Radio Technologies and Concepts for IMT-Advanced*, Wiley, 2009.
- [26] European Telecommunications Standards Institute, "LTE; Evolved Universal Terrestrial Radio Access (E-UTRA); Radio Frequency (RF) requirements for LTE Pico Node B," Technical Report, ETSI TR 136 931 V9.0.0, 2011.
- [27] E.L. Crow and K. Shimizu, *Lognormal Distributions: Theory and Application*, CRC Press, 1987.
- [28] P. Dent, G.E. Bottomley, and T. Croft, "Jakes fading model revisited," *Electronics Letters*, vol. 29, no. 13, pp. 1162–1163, 1993.
- [29] E.P. Caspers, S.H. Yeung, T.K. Sarkar, A. Garcia-Lamperez, M.S. Palma, M.A. Lagunas, and A. Perez-Neira, "Analysis of information and power transfer in wireless communications," *IEEE Antennas and Propagation Magazine*, vol. 55, no. 3, pp. 82–95, 2013.
- [30] D. Defays, "An efficient algorithm for a complete link method," *Computer J.*, vol. 20, no. 4, pp. 364–366, 1976.
- [31] J. Han and M. Kamber, *Data Mining: Concepts and Techniques*, Academic Press, 2001.

- [32] C.E. Shannon, "A mathematical theory of communication," *Bell System Technical J.*, vol. 27, pp. 379–423, 1948.
- [33] A.J. Goldsmith and S. G. Chua, "Variable-rate variable-power MQAM for fading channels," *IEEE Trans. Comm.*, vol. 45, no. 10, pp. 1218–1230, 1997.
- [34] Y.C. Wang, Y.F. Chen, and Y.C. Tseng, "Using rotatable and directional (R&D) sensors to achieve temporal coverage of objects and its surveillance application," *IEEE Trans. Mobile Computing*, vol. 11, no. 8, pp. 1358–1371, 2012.
- [35] L. Chen, Y. Huang, F. Xie, Y. Gao, L. Chu, H. He, Y. Li, F. Liang, and Y. Yuan, "Mobile relay in LTE-advanced systems," *IEEE Comm. Magazine*, vol. 51, no. 11, pp. 144–151, 2013.
- [36] J. Kokkonen, J. Ylitalo, P. Luoto, S. Scott, J. Leinonen, and M. Latva-aho, "Performance evaluation of vehicular LTE mobile relay nodes," *Proc. IEEE Int'l Symp. Personal Indoor and Mobile Radio Comm.*, 2013, pp. 1972–1976.
- [37] W. Debus, "RF path loss & transmission distance calculations," Axonn Technical Memorandum, 2006.
- [38] A.S. Hamza, S.S. Khalifa, H.S. Hamza, and K. Elsayed, "A survey on inter-cell interference coordination techniques in OFDMA-based cellular networks," *IEEE Comm. Surveys & Tutorials*, vol. 15, no. 4, pp. 1642–1670, 2013.